Open Journal of Fluid Dynamics, 2026, 16(3), 91-102
https://www.scirp.org/journal/ojfd
ISSN Online: 2165-3860
ISSN Print: 2165-3852

Free Convection in a Isoceles Triangular Cavity Filled with a Darcy-Brinkman Porous Medium: Effect of Darcy and Prandtl Numbers

Giovani Elie Baptista Malomar, Samba Dia, Omar Ngor Thiam, Cheikh Mbow

Department of Physics, Faculty of Science and Technology, University Cheikh Anta Diop, Dakar, Senegal
Email: giovanielie.malomar@ucad.edu.sn, samba.dia@ucad.edu.sn, omarngor.thiam@ucad.edu.sn, mbowy@yahoo.com

How to cite this paper: Malomar, G.E.B., Dia, S., Thiam, O.N. and Mbow, C. (2026) Free Convection in a Isoceles Triangular Cavity Filled with a Darcy-Brinkman Porous Medium: Effect of Darcy and Prandtl Numbers. *Open Journal of Fluid Dynamics*, **16**, 91-102.
https://doi.org/10.4236/ojfd.2026.163006

Received: December 2, 2025
Accepted: September 14, 2026
Published: September 17, 2026

Abstract

In this article, we investigate the effects of the Darcy and Prandtl numbers on steady-state natural convection in an isoceles porous triangular cavity whose horizontal base is partially heated and whose upper walls are cooled. The uniform heat source is located centrally at the base wall. The isosceles triangular geometry directly simulates the attics of buildings. This model is widely used to optimise thermal insulation in the building sector. Darcy-Brinkman model is used. It is also assumed the fluid used is incompressible and obeys the Boussinesq approximation. The non-dimensionless governing equations, stream function-vorticity, momentum and energy are discretized by finite difference method and solved using the successive over-relaxation (SOR) method. Streamline and isotherm patterns were presented at different, length of heater $\epsilon = 0.5$, Darcy number ($10^{-4} \le Da \le 10^{-2}$), Prandtl number ($0.7 \le Pr \le 7$) and for different Rayleigh number ($10^{3} \le Ra \le 10^{6}$). On the basis of the results, it is observed that the Darcy number has an effect on both the initiation of convection and the average Nusselt number. The critical Rayleigh number where convection becomes the dominant heat transfer mode decreases significantly with increasing Darcy number. The mean Nusselt number increases with increasing Darcy number. The Prandtl number has a limited effect on overall heat transfer in the present system, for the range of values used.

Keywords

Free Convection, Numerical Study, Partially Heating, Darcy and Prandtl Numbers

1. Introduction

The natural convection in confined porous media saturated by fluid is fundamental in the fields of engineering and physics. This interest arises from the importance of this heat transfer mode in various engineering fields such as storage of the thermal energy, solar energy collectors, thermal design for the buildings, cooling of electronic components (Alves *et al.* [1]; Kuznetsov *et al.* [2]; Sheremet *et al.* [3]), the underground spread of pollutants (Bagchi *et al.* [4]). The literature on the convective flow in porous media is abundant. An excellent review of most of these studies is in the books (Nield *et al.* [5]; Pop *et al.* [6]; Vafai [7]; Ingham *et al.* [8]) that give a complete overview of the current state of research in this area.

In many studies, rectangular enclosures have been chosen for the study of natural convection in both fluid and porous media. In addition to rectangular cavities, triangular cavities are of paramount importance in many applications, particularly in the building industry. Triangular cavities filled with air have been studied to simulate thermo-convective transfers in buildings [9]-[14].

Other, more recent studies focus on the dynamics of entrained cavities. In [15] [16], the authors approach flow control from very different perspectives. In [15], the authors favour a dynamic and analytical approach, demonstrating how an external force (the magnetic field) can slow down and structure viscous flow, whilst in [16], they adopt a purely kinematic approach, exploring the behavioural limits of a fluid subjected to movement constraints imposed across all its boundaries.

However, the number of studies on triangular cavities filled with a porous medium is limited and generally focuses on right-angled triangular cavities [17]-[20], with Darcy's model often being used. These studies have highlighted the impact of the cavity's aspect ratio and Rayleigh number. In our work, we examine natural convection in isosceles triangular cavities. A few studies have been conducted in such a configuration [21]-[25].

Malomar *et al.* [21] provides essential quantitative clarification on the optimisation of heat source dimensions in porous media under the Darcy-Brinkman model. It demonstrates that a restricted source improves the relative efficiency of convective heat transfer at high Rayleigh numbers.

Basak *et al.* [22] used finite element analysis to study the effects of uniform and non-uniform heating of the base wall on natural convection flows in isosceles triangular enclosures filled with porous media. The detailed analysis was performed in two cases based on different thermal boundary conditions: (1) two inclined walls are maintained at a constant cold temperature while the bottom wall is uniformly heated; (2) two inclined walls are maintained at a constant cold temperature while the bottom wall is heated non-uniformly. The numerical results are presented in terms of current functions, temperature profiles, and Nusselt numbers. It is observed that for small Darcy numbers, heat transfer is mainly due to conduction regardless of Pr. As the Darcy number increases, there is a shift from the dominant conduction regime to the dominant convection regime. Non-uniform heating of the lower wall produces a higher heat transfer rate at the center of the lower wall than uniform heating, but the average Nusselt number indicates a lower overall heat transfer rate for non-uniform heating.

In [23], Basak *et al.* investigate numerically, the phenomena of natural convection in an isosceles triangular enclosure filled with a porous matrix. A penalty finite element analysis with bi-quadratic elements is used for solving the Navier-Stokes and energy balance equations. The detailed study is carried out in two cases depending on various thermal boundary conditions; case I: two inclined walls are uniformly heated while the bottom wall is isothermally cooled and case II: two inclined walls are non-uniformly heated while the bottom wall is isothermally cooled. It has been found that at low Darcy numbers, the heat transfer is primarily due to conduction irrespective of the Ra and Pr. As Rayleigh number increases, there is a change from conduction dominant region to convection dominant region for ($Da = 10^{-3}$), and the critical Rayleigh number corresponding to on-set of convection is obtained. Some interesting features of stream function and isotherm contours are discussed especially for low and high Prandtl number limits.

Varol *et al.* [24] examined heat transfer by natural convection in triangular enclosures filled with porous media and subjected to different boundary conditions. Six different cases were tested based on all possible boundary conditions for temperature on the vertical, bottom, and inclined walls of the enclosure. Based on the results, they observed that when the heating device was located on the bottom wall, multiple vortices formed, and the highest heat transfer was achieved compared to the other cases.

In [25], Varol *et al.* investigated numerical analysis of the entropy production has been performed due to natural convection heat transfer and fluid flow in isosceles triangular enclosures with partially heated from below and symmetrically cooled from sloping walls. It is observed that entropy production number increases but Bejan number decreases with increasing of Rayleigh number. However, both entropy production due to heat transfer and fluid friction irreversibility are affected by higher inclination angle of triangle and length of heater.

The main objective of this study is to numerically examine the effects of natural convection within a porous isocele triangular cavity subjected to localized heat source. The Darcy-Brinkman model in the Boussinesq approximation is used to model the flow within the porous medium. The influences of the Darcy number, Prandtl number, and Rayleigh number were studied.

2. Materials and Methods

2.1. Basic Equations

A schematic geometry of the problem is shown in **Figure 1**, where x' and y' are the cartesian coordinates, H' is the height of the cavity, L' the length of the base of the cavity and ϵ' the length of heater isothermal source. This is a triangular porous cavity two-dimensional and the rest of the non-heated portions of the base wall are assumed to be thermally adiabatic. All walls of the cavity are assumed to be impermeable. At the same, bottom wall is partially or completely heated with a centrally located isothermal heat source T'_h and inclined walls are isothermally cooled at a constant temperature T'_c. The Boussinesq approximation is employed. Isotropy, homogeneity and local thermal equilibrium in the porous medium are assumed.

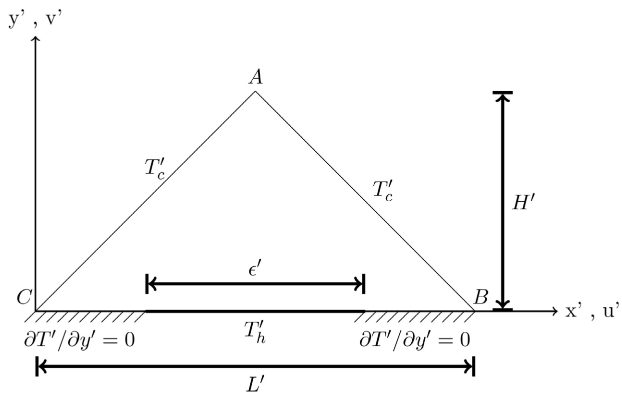

Figure 1. Schematic diagram of the physical model and coordinate system.

Under these assumptions, the dimensionless forms of governing equations for steady free convection flow in porous medium are (see Nield and Bejan [5]):

$$\frac{\partial^2 \psi}{\partial x^2} + \frac{\partial^2 \psi}{\partial y^2} = -\omega \tag{1}$$

$$\frac{\partial \psi}{\partial y}\frac{\partial \omega}{\partial x} - \frac{\partial \psi}{\partial x}\frac{\partial \omega}{\partial y} = \phi Pr\left(\frac{\partial^2 \omega}{\partial x^2} + \frac{\partial^2 \omega}{\partial y^2}\right) - \frac{\phi^2 Pr}{Da}\omega + Ra\phi^2 Pr\frac{\partial T}{\partial x} \tag{2}$$

$$\frac{\partial \psi}{\partial y}\frac{\partial T}{\partial x} - \frac{\partial \psi}{\partial x}\frac{\partial T}{\partial y} = \frac{\partial^2 T}{\partial x^2} + \frac{\partial^2 T}{\partial y^2} \tag{3}$$

where the Rayleigh, Darcy and Prandtl numbers are:

$$Ra = \frac{g\beta L'^3\left(T'_h - T'_c\right)}{\nu\alpha} \tag{4}$$

$$Da = \frac{K}{L'^2} \tag{5}$$

$$Pr = \frac{\nu}{\alpha} \tag{6}$$

The relationships between the dimensionless variables of equations (Equations (1) - (3)) and their dimensional counterparts are:

$$(x, y) = \left(\frac{x'}{L'}, \frac{y'}{L'}\right); \quad (u, v) = \left(\frac{u'L'}{\alpha}, \frac{v'L'}{\alpha}\right); \quad T = \frac{T' - T'_c}{T'_h - T'_c} \tag{7}$$

The relationships between dimensionless stream fuction, ψ, vorticity, ω and velocity components u and v are:

$$\omega = \frac{\partial v}{\partial x} - \frac{\partial u}{\partial y} \tag{8}$$

$$u = \frac{\partial \psi}{\partial y} \text{ and } v = -\frac{\partial \psi}{\partial x} \tag{9}$$

Equations (1) - (3) are associated with the following dimensionless boundary conditions:

$$\begin{cases} \psi = 0;\ \omega = 0;\ T = 0 \text{ initial conditions} \\ \psi = 0 \text{ on three side} \\ T = T_c = 0 \text{ on side } AB \text{ and } AC \\ T = T_h = 1 \text{ for } \frac{1-\epsilon}{2} \le x \le \frac{1+\epsilon}{2} \text{ on } BC \\ \frac{\partial T}{\partial y} = 0 \text{ for } 0 \le x \le \frac{1-\epsilon}{2} \text{ and } \frac{1+\epsilon}{2} \le x \le 1 \text{ on } BC \end{cases} \tag{10}$$

where ϵ is the dimensionless heat source length, defined by $\epsilon = \frac{\epsilon'}{L'}$.

For calculate the vorticity values at the boundary points we use Thom's formula in Weinan *et al.* [26].

Heat Transfer

Once as the temperature field is known, we may define the heat transfer coefficient in terms of local Nusselt number, Nu from the heated portion of the base wall by

$$Nu = -\left(\frac{\partial T}{\partial y}\right)_{y=0} \tag{11}$$

However, this local Nu is unbounded at the corners of triangular cavity where the hot base meets the cold side walls when the bottom wall is completely heated. Therefore, determination of an average Nu characterizing the heat transfer would be unbounded at the tip region.

On the hot wall, the average Nusselt number is determined by:

$$\overline{Num} = -\int_{\frac{1-\epsilon}{2}}^{\frac{1+\epsilon}{2}} \left(\frac{\partial T}{\partial y}\right)_{y=0} \mathrm{d}x \tag{12}$$

2.2. Numerical Method

The governing equations (Equations (1) - (3)) associated with the boundary conditions (Equation (10)) are discretized by a finite difference scheme, centred and forward accurate to the second order and first order, respectively. The three equations in stream fuction-vorticity and temperature formulation are then solved using successive over-relaxation (SOR) method. We note that, we have used the same relaxation parameter when we update the stream function, vorticity and temperature values. Uniform grids have been selected in both the x and y direction. We have developed a numerical code with Fortran 95.

During iterations, the calculation stops when between two iterations, the following conditions are satisfied by the stream function, vorticity and temperature:

$$\max\left(\left|R_\psi\right|\right) \le 10^{-8} \text{ and } \max\left(\left|R_\omega\right|\right) \le 10^{-5} \text{ and } \max\left(\left|R_T\right|\right) \le 10^{-8} \tag{13}$$

Here, R_ψ, R_ω and R_T are the residual of the steady state stream function, vorticity and temperature equations (Equations (1) - (3)). We define this residual as the following:

$$R_\psi = \frac{\psi_{i+1,j} - 2\psi_{i,j} + \psi_{i-1,j}}{\Delta x^2} + \frac{\psi_{i,j+1} - 2\psi_{i,j} + \psi_{i,j-1}}{\Delta y^2} + \omega_{i,j} \tag{14}$$

$$\begin{aligned} R_\omega = {} & \phi Pr\left(\frac{\omega_{i+1,j} - 2\omega_{i,j} + \omega_{i-1,j}}{\Delta x^2} + \frac{\omega_{i,j+1} - 2\omega_{i,j} + \omega_{i,j-1}}{\Delta y^2}\right) \\ & - \frac{\phi^2 Pr}{Da}\omega_{i,j} + Ra\phi^2 Pr\left(\frac{T_{i+1,j} - T_{i-1,j}}{2\Delta x}\right) \\ & + \frac{\left(\psi_{i+1,j} - \psi_{i-1,j}\right)\left(\omega_{i,j+1} - \omega_{i,j-1}\right)}{4\Delta x\Delta y} \\ & + \frac{\left(\psi_{i,j-1} - \psi_{i,j+1}\right)\left(\omega_{i+1,j} - \omega_{i-1,j}\right)}{4\Delta x\Delta y} \end{aligned} \tag{15}$$

$$\begin{aligned} R_T = {} & \frac{T_{i+1,j} - 2T_{i,j} + T_{i-1,j}}{\Delta x^2} + \frac{T_{i,j+1} - 2T_{i,j} + T_{i,j-1}}{\Delta y^2} \\ & + \frac{\left(\psi_{i+1,j} - \psi_{i-1,j}\right)\left(T_{i,j+1} - T_{i,j-1}\right)}{4\Delta x\Delta y} \\ & + \frac{\left(\psi_{i,j-1} - \psi_{i,j+1}\right)\left(T_{i+1,j} - T_{i-1,j}\right)}{4\Delta x\Delta y} \end{aligned} \tag{16}$$

Preliminary tests on the influence of the mesh have allowed us to retain a uniform mesh size of 120 × 60 for all simulation except simulation at high darcy ($Da = 10^{-2}$) where we used 200 × 100. The present numerical code has been validated against the works of Basak *et al.* [22].

3. Results and Discussion

Symmetric flow and temperature field

In the field of control parameters of the problem cited above, we have noticed that the computed flow and temperature field remains symmetric with respect to the geometric midplane (see figures in [21]). The flow rises in the center of the cavity and falls along each cold inclined side creating mirror image structures that rotate clockwise in the right half and counterclockwise in the left half. It is noted that the horizontal component of velocity is zero everywhere along the vertical centerline of the cavity. This work builds on the research carried out by Malomar *et al.* in [21] and, for the sake of convenience, the figures showing the hydrodynamic and thermal fields have not been included.

Darcy number effect

In the present study, three Darcy numbers are considered: $Da = 10^{-4}$, $Da = 10^{-3}$ and $Da = 10^{-2}$. Throughout this section the size of the heat source is $\epsilon = 0.5$.

By comparing the fluid flow and thermal behavior for the different Darcy numbers considered in this study, we observe that there is no great difference between them when $Ra = 10^3$. However, flow velocities increase with increasing Da. This can be explained by the fact that a porous medium with a high Darcy number offers lower resistance to fluid movement and therefore allows higher flow velocities. The structural analysis of the temperature field shows that heat transfer is dominated by conduction at $Ra = 10^3$.

For $Da = 10^{-4}$, we note that for the Ra range used, heat transfer is mainly by conduction. As Ra increases to to 10^4, a convective flow regime dominates for $Da = 10^{-3}$ and $Da = 10^{-2}$. Flow velocities increase, and a thermal plume is observed at $Da = 10^{-2}$ and the beginning of plume formation at $Da = 10^{-3}$. As the Darcy number increases to $Da = 10^{-2}$, significant changes are observed beyond $Ra = 10^3$. As Ra increases, the intensity of the flow increases and the convective cells acquire a quasi-triangular shape. The thermal gradients show an increasingly narrow thermal plume.

The global heat transfer results for the different Darcy numbers are shown in Figure 2. As can be seen, the Darcy number has an effect both on the onset of convection and on the average Nusselt number beyond the critical point. An interesting aspect was noted: for the Da parameter range used, the critical Rayleigh number where convection becomes the dominant heat transfer mode decreases significantly with increasing Da. We also noted that the average Nusselt number remains virtually constant when the conductive mode dominates, regardless of the Darcy number, as the size of the heating source is kept fixed. It should be noted that beyond a certain Ra the average Nusselt number increases with increasing Da. This result is to be expected, since for higher Da numbers, the porous medium offers low resistance to fluid movement which causes increasing convective heat transfer. The temperature profiles along the axis of symmetry of the cavity, shown in Figure 3 also indicate that the temperature distribution varies significantly from one Darcy number to the other.

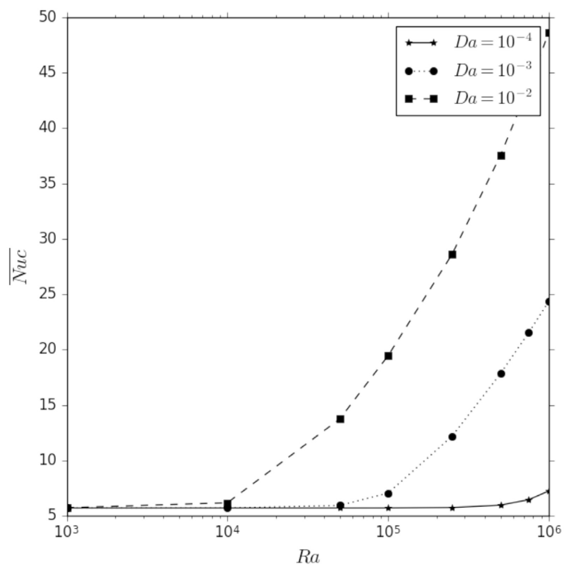

Figure 2. Evolution of $\overline{Nuc}$ as a function of Ra for different Da, $Pr = 7$.

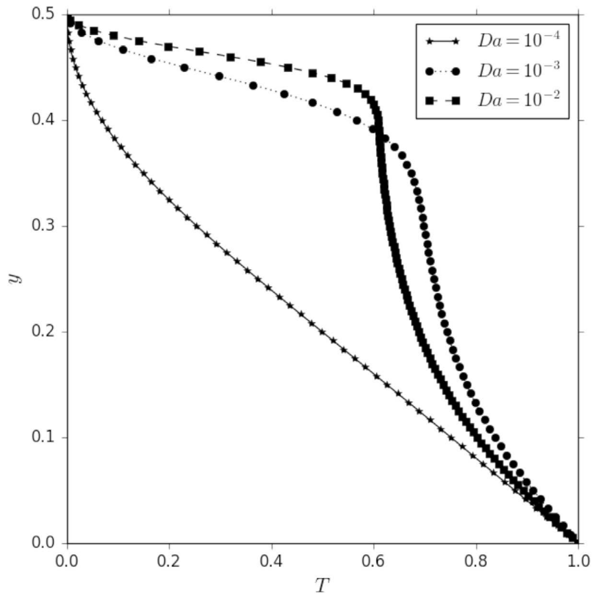

Figure 3. Temperature profile along the vertical axis of cavity symmetry for different Da, $Ra = 5\times10^5$, $Pr = 7$.

Effect of Prandtl number

In the present study, two different values of Prandtl number are considered: $Pr = 0.7$ et $Pr = 7$. They are approximately equal to the Prandtl numbers of air ($Pr = 0.71$ à 25˚C) and water ($Pr = 6.26$ à 25˚C). These fluids were chosen for two main reasons. On the one hand, they are generally used in many studies of convection in fluid or porous media, and so there are several available in the literature to serve as a basis for comparison. On the other hand, for these two fluids, there is no significant change of their viscosity with temperature, and consequently of their Prandtl number.

An analysis of the flow patterns and temperature distributions reveals that for the range of Prandtl numbers used, for a given Ra, the hydrodynamic structures remain remarkably similar, as do the thermal fields. At $Ra = 10^3$, two slightly rotating cells are observed, and the flow velocities are identical. The thermal field confirm that the dominant mode of heat transfer is conduction. As Ra increases, flow velocities increase and the temperature distribution indicates the rise of an increasingly narrow thermal plume, confirming that the dominant heat transfer mode is convection. Global heat transfer results for different Prandtl numbers are shown in Figure 4. As can be seen, the two curves overlap perfectly, indicating that the Prandtl number has a limited effect on the overall heat transfer of the system. These results are in line with those found in both the Rayleigh-Benard and Horton-Rogers-Lapwood problems.

The temperature profiles along the central line of symmetry, shown in Figure 5, show no difference between the two systems. Based on the above arguments, we can conclude that the Prandtl number is a non-significant parameter in determining the global heat transfer characteristics in the present system.

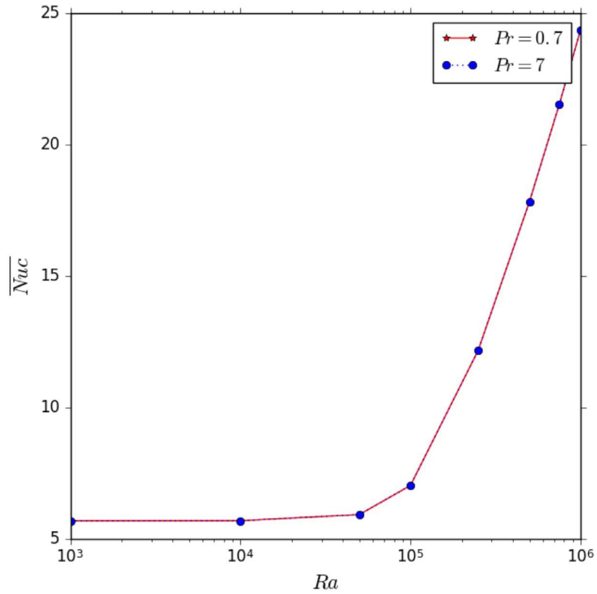

Figure 4. Evolution of $\overline{Nuc}$ as a fonction of Ra for different Pr, $Da=10^{-3}$.

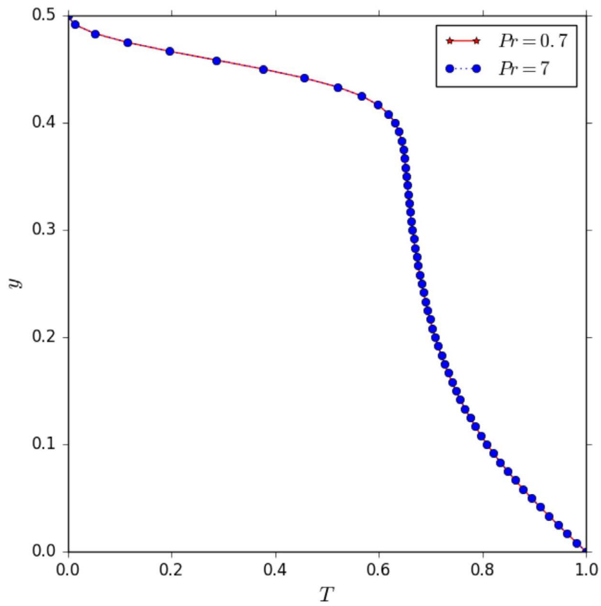

Figure 5. Temperature profile along the vertical axis of cavity symmetry for different Pr, $Ra=10^6$, $Da=10^{-3}$.

4. Conclusion

This study investigated the numerical analysis of natural laminar convection within a porous isocele triangular cavity subjected to localized heat source ($\epsilon = 0.5$). The Darcy-Brinkman model in the Boussinesq approximation was used to model the flow within the porous medium. The influences of the Darcy number, the Prandtl number, and the Rayleigh number were studied. The main conclusions are as follows:

- It is observed that the Darcy number has an effect on both the onset of convection and the average Nusselt number. The critical Rayleigh number at which convection becomes the dominant mode of heat transfer decreases significantly with increasing Darcy number.
- The average Nusselt number increases with increasing Darcy number.
- The Prandtl number has a limited effect on overall heat transfer in the present system.

Acknowledgements

We thank the Editor and the reviewers for their comments.

Author Contributions

All the authors contributed to writing and stabilising the numerical code and to analysing the results.

Conflicts of Interest

The authors declare no conflicts of interest regarding the publication of this paper.

References

[1] Alves, T.A. and Altemani, C.A.C. (2012) An Invariant Descriptor for Heaters Temperature Prediction in Conjugate Cooling. *International Journal of Thermal Sciences*, **58**, 92-101. https://doi.org/10.1016/j.ijthermalsci.2012.03.007

[2] Kuznetsov, G.V. and Sheremet, M.A. (2008) New Approach to the Mathematical Modeling of Thermal Regimes for Electronic Equipment. *Russian Microelectronics*, **37**, 131-138. https://doi.org/10.1134/s1063739708020078

[3] Sheremet, M.A. and Pop, I. (2014) Natural Convection in a Square Porous Cavity with Sinusoidal Temperature Distributions on Both Side Walls Filled with a Nanofluid: Buongiorno's Mathematical Model. *Transport in Porous Media*, **105**, 411-429. https://doi.org/10.1007/s11242-014-0375-7

[4] Bagchi, A. and Kulacki, F.A. (2013) Natural Convection in Superposed Fluid-Porous Layers. Springer Briefs in Applied Sciences and Technology. Springer.

[5] Nield, D.A. and Bejan, A. (2017) Convection in Porous Media, Volume 3. Springer.

[6] Pop, I. and Ingham, D.B. (2001) Convective Heat Transfer: Mathematical and Computational Modelling of Viscous Fluids and Porous Media. Pergamon.

[7] Vafai, K. (2015) Handbook of Porous Media. CRC Press.

[8] Ingham, D.B. and Pop, I. (2005) Transport Phenomena in Porous Media III. Elsevier.

[9] Asan, H. and Namli, L. (2000) Laminar Natural Convection in a Pitched Roof of Triangular Cross-Section: Summer Day Boundary Conditions. *Energy and Buildings*, **33**, 69-73. https://doi.org/10.1016/s0378-7788(00)00066-9

[10] Holtzman, G.A., Hill, R.W. and Ball, K.S. (2000) Laminar Natural Convection in Isosceles Triangular Enclosures Heated from Below and Symmetrically Cooled from Above. *Journal of Heat Transfer*, **122**, 485-491. https://doi.org/10.1115/1.1288707

[11] Asan, H. and Namli, L. (2001) Numerical Simulation of Buoyant Flow in a Roof of Triangular Cross-Section under Winter Day Boundary Conditions. *Energy and Buildings*, **33**, 753-757. https://doi.org/10.1016/s0378-7788(01)00063-9

[12] Akinsete, V.A. and Coleman, T.A. (1982) Heat Transfer by Steady Laminar Free Convection in Triangular Enclosures. *International Journal of Heat and Mass Transfer*, **25**, 991-998. https://doi.org/10.1016/0017-9310(82)90074-6

[13] Ridouane, E.H., Campo, A. and Hasnaoui, M. (2006) Benefits Derivable from Connecting the Bottom and Top Walls of Attic Enclosures with Insulated Vertical Side Walls. *Numerical Heat Transfer*, *Part A*: *Applications*, **49**, 175-193. https://doi.org/10.1080/10407780500302257

[14] Kpode, K., Sow, M.L. and Mbow, C. (2016) Unsteady Natural Convection with Summer Boundary Conditions in a Habitat at High Rayleigh Number and at High Time. *Energy and Buildings*, **121**, 72-77. https://doi.org/10.1016/j.enbuild.2016.03.068

[15] Turkyilmazoglu, M. and Alotaibi, A. (2025) Analysis of MHD Stokes Fluid Flow in a Cavity Driven by Moving Parallel Lid(s). *Theoretical and Computational Fluid Dynamics*, **39**, Article No. 31. https://doi.org/10.1007/s00162-025-00750-4

[16] Turkyilmazoglu, M. and Alotaibi, A. (2024) Fluid Motion in a Cavity Driven by a Four-Sided Moving Lid with Uniform Velocity. *European Journal of Mechanics—B*/*Fluids*, **107**, 67-79. https://doi.org/10.1016/j.euromechflu.2024.06.004

[17] Poulikakos, D. and Bejan, A. (1983) Numerical Study of Transient High Rayleigh Number Convection in an Attic-Shaped Porous Layer. *Journal of Heat Transfer*, **105**, 476-484. https://doi.org/10.1115/1.3245610

[18] Varol, Y., Oztop, H.F. and Varol, A. (2007) Natural Convection in Porous Triangular Enclosures with a Solid Adiabatic Fin Attached to the Horizontal Wall. *International Communications in Heat and Mass Transfer*, **34**, 19-27. https://doi.org/10.1016/j.icheatmasstransfer.2006.09.004

[19] Varol, Y., Oztop, H.F. and Varol, A. (2007) Free Convection in a Triangular Porous Media Filled Enclosure Heated or Cooled Horizontal and Vertical Walls. *The* 3*rd International Energy*, *Exergy and Environment Symposium* (*IEEE*3), Évora, 1-5 July 2007.

[20] Varol, Y., Oztop, H.F. and Varol, A. (2006) Free Convection in Porous Media Filled Right-Angle Triangular Enclosures. *International Communications in Heat and Mass Transfer*, **33**, 1190-1197. https://doi.org/10.1016/j.icheatmasstransfer.2006.08.008

[21] Malomar, G.E.B., Thiam, O.N. and Mbow, C. (2025) Numerical Solutions of 2-D Laminar Free Convection in an Isoceles Triangular Cavity Filled with a Darcy-Brinkman Porous Medium: Effect of Heat Source Size. *Open Journal of Fluid Dynamics*, **15**, 222-235. https://doi.org/10.4236/ojfd.2025.154013

[22] Basak, T., Roy, S. and Krishna Babu, S. (2008) Natural Convection and Flow Simulation in Differentially Heated Isosceles Triangular Enclosures Filled with Porous Medium. *Chemical Engineering Science*, **63**, 3328-3340. https://doi.org/10.1016/j.ces.2008.03.038

[23] Basak, T., Roy, S., Babu, S.K. and Pop, I. (2008) Finite Element Simulations of Natural Convection Flow in an Isosceles Triangular Enclosure Filled with a Porous Medium: Effects of Various Thermal Boundary Conditions. *International Journal of Heat and Mass Transfer*, **51**, 2733-2741. https://doi.org/10.1016/j.ijheatmasstransfer.2007.10.009

[24] Varol, Y., Oztop, H.F. and Varol, A. (2008) Free Convection Heat Transfer and Flow Field in Triangular Enclosures Filled with Porous Media. *Journal of Porous Media*, **11**, 103-115. https://doi.org/10.1615/jpormedia.v11.i1.70

[25] Varol, Y., Oztop, H.F. and Koca, A. (2008) Entropy Production Due to Free Convection in Partially Heated Isosceles Triangular Enclosures. *Applied Thermal Engineering*, **28**, 1502-1513. https://doi.org/10.1016/j.applthermaleng.2007.08.013

[26] Weinan, E. and Liu, J.G. (1996) Vorticity Boundary Condition and Related Issues for Finite Difference Schemes. *Journal of Computational Physics*, **124**, 368-382. https://doi.org/10.1006/jcph.1996.0066

Nomenclature

g	Gravity intensity, m·s^{-2}
K	Permeability of the porous medium, m^2
T	Dimensionless temperature
(x, y)	Dimensionless coordinates
(u, v)	Dimensionless velocitu components along x and y axes
Ra	Rayleigh number for porous medium
Da	Darcy number
Pr	Prandtl number
Nu	local Nusselt number, at the heated base wall
$\overline{Nuc}$	Average Nusselt number, at the heated base wall

Greek Symbols

α	Effective thermal diffusivity, m^2·s^{-1}
β	Coefficient of thermal expansion, K^{-1}
ν	kinematic viscosity, kg·m^{-1}·s^{-1}
ϕ	Porosity of porous media
ϵ	dimensionless heat source length ω Vorticity
ψ	Dimensionless stream function
ρ_0	Reference density of fluid, kg·m^{-3}

Superscript

(ʹ)	Dimensional variables
(-)	Average values

Subscript

c	Cold
h	Hot